


The two-component system histidine kinase EnvZ contributes to Avian pathogenic *Escherichia coli* pathogenicity by regulating biofilm formation and stress responses

Dandan Fu ^{*,†}, Jianmei Wu,^{*,†} Xiaoyan Wu,^{*,†} Ying Shao,^{*,†} Xiangjun Song,^{*,†} Jian Tu,^{*,†} and Kezong Qi^{*,†,1}

^{*}Anhui Province Key Laboratory of Veterinary Pathobiology and Disease Control, College of Animal Science and Technology, Anhui Agricultural University, Hefei, Anhui 230036, PR China; and [†]Anhui Province Engineering Laboratory for Animal Food Quality and Bio-Safety, College of Animal Science and Technology, Anhui Agricultural University, Hefei, Anhui 230036, PR China

ABSTRACT EnvZ, the histidine kinase (HK) of OmpR/EnvZ, transduces osmotic signals in *Escherichia coli* K12 and affects the pathogenicity of *Shigella flexneri* and *Vibrio cholera*. Avian pathogenic *E. coli* (APEC) is an extra-intestinal pathogenic *E. coli* (ExPEC), causing acute and sudden death in poultry and leading to severe economic losses to the global poultry industry. How the functions of EnvZ correlate with APEC pathogenicity was still unknown. In this study, we successfully constructed the *envZ* mutant strain AE17 Δ *envZ* and the inactivation of *envZ* significantly reduced biofilms and altered red, dry, and rough (rdar) morphology. In addition, AE17 Δ *envZ* was significantly less resistant to acid, alkali, osmotic, and oxidative stress conditions. Deletion of *envZ* significantly enhanced sensitivity to specific pathogen-free (SPF) chicken serum and increased adhesion to chicken embryonic fibroblast

DF-1 cells and elevated inflammatory cytokine IL-1 β , IL6, and IL8 expression levels. Also, when compared with the WT strain, AE17 Δ *envZ* attenuated APEC pathogenicity in chickens. To explore the molecular mechanisms underpinning *envZ* in APEC17, we compared the WT and *envZ*-deletion strains using transcriptome analyses. RNA-Seq results identified 711 differentially expressed genes (DEGs) in the *envZ* mutant strain and DEGs were mainly enriched in outer membrane proteins, stress response systems, and TCSs. Quantitative real-time reverse transcription PCR (RT-qPCR) showed that EnvZ influenced the expression of biofilms and stress responses genes, including *ompC*, *ompT*, *mtrA*, *basR*, *hdeA*, *hdeB*, *adiY*, and *uspB*. We provided compelling evidence showing EnvZ contributed to APEC pathogenicity by regulating biofilms and stress response expression.

Key words: avian pathogenic *Escherichia coli*, histidine kinase EnvZ, biofilms, stress responses, pathogenicity

2023 Poultry Science 102:102388

<https://doi.org/10.1016/j.psj.2022.102388>

INTRODUCTION

Avian pathogenic *Escherichia coli* (APEC), one of the extra-intestinal pathogenic *E. coli* (ExPEC) with a broad host spectrum, is a serious threat to poultry industry development and one of the main causes of morbidity and mortality in birds (Moulin-Schouleur et al., 2007; Kathayat et al., 2021). In APEC, there are several two-component systems (TCSs), including UvrY/BarA, CpxR/A, PhoP/Q, OmpR/EnvZ, BasR/S, and QseB/C, which help bacteria adapt to complex external

environments and exert pathogenic effects (Oshima et al., 2002; Gotoh et al., 2010; Cai et al., 2013; Breland et al., 2017; Tiwari et al., 2017). A typical TCS contains a histidine kinase (HK) to receive external input signals and a response regulator (RR) to transmit signals. The HK detects many environmental stimuli which are transferred to homologous RRs via autophosphorylation and catalytic phosphorylation (Tokishita et al., 1991; Mascher et al., 2006; Gotoh et al., 2010; Gushchin et al., 2017). Studies have indicated histidine kinases have been found to play an important role in the TCSs and the regulation of APEC pathogenesis. QseC, a bifunctional sensor kinase, controls the phosphorylation state of QseB and contributes to APEC virulence and innate immunity (Chaudhari and Kariyawasam, 2014). The UvrY/BarA HK BarA is involved in DF-1 cell adhesion and invasion,

© 2022 The Authors. Published by Elsevier Inc. on behalf of Poultry Science Association Inc. This is an open access article under the CC BY-NC-ND license (<http://creativecommons.org/licenses/by-nc-nd/4.0/>).

Received May 18, 2022.

Accepted December 1, 2022.

¹Corresponding author: qkz@ahau.edu.cn

serum resistance, and APEC virulence (Herren et al., 2006). CpxA is a sensor kinase of the CpxR/A stress response system and is required for adherence, invasion, motility, and the production of type I fimbriae and biofilms in APEC (Matter et al., 2018). Thus, TCS HKs are key regulators that mediate bacterial responses to environmental changes to establish pathogen infection.

EnvZ, the histidine kinase of OmpR/EnvZ TCS, consists of 450 amino acid residues and has 2 transmembrane helices: a periplasmic structural domain and a cytoplasmic structural domain (Tokishita et al., 1991; Khorchid et al., 2005). When stimulated, EnvZ senses changes in osmotic pressure through its cytoplasmic structural domain, causing autophosphorylation at His-243 and later transferring the phosphate group to OmpR, with OmpR-P binding to outer membrane protein genes and responding to osmotic stress (Tiwari et al., 2017). In *E. coli* K12, EnvZ binds to the inner membrane protein MzrA and responds to environmental signals (Gerken et al., 2009). In *Shigella flexneri*, EnvZ regulates vir expression and affects the invasion of Hela cells (Bernardini et al., 1990). In *Vibrio cholerae*, EnvZ is required for virulence during infant mouse intestinal colonization (Xi et al., 2020).

Since EnvZ has been well characterized as an important factor in other Gram-negative bacteria, in this study, we evaluated the biological and virulence properties of *envZ* in APEC. We explored the function of EnvZ in APEC pathogenesis and showed EnvZ participated in biofilm formation, curli production, responses to environmental stresses (including acid, alkali, osmotic, and oxidative), serum resistance, and APEC pathogenicity. Transcriptomic studies showed EnvZ affected bacterial virulence genes and helped regulate several important biological processes, including microbial metabolism in diverse environments, biofilm formation, and other TCSs. All in all, we proved that the TCS histidine kinase EnvZ plays a key role in APEC pathogenicity, and provides potential drug targets for the treatment and prevention of APEC infection.

MATERIALS AND METHODS

Bacterial Strains, Plasmids, and Growth Conditions

The APEC17 strain is a serotype O2 strain isolated from a case of avian colibacillosis in Anhui Province, China (Tu et al., 2016). All strains and plasmids are listed in Table 1. Bacterial strains were grown in Luria-Bertani (LB) medium (Sangon, Shanghai, China) at 28°C or 37°C. If required, antibiotics were added at the following concentrations: ampicillin (100 µg/mL) and chloramphenicol (30 µg/mL) (Sangon).

Construction of the *envZ* Mutant and Complement Strains

The mutant strain AE17Δ*envZ* was constructed from the wild-type (WT) AE17 using λ-red recombination

Table 1. Strains and plasmids used in this study.

Strains	Relevant genotype	Source
AE17	APEC wild-type strain	Laboratory stock
AE17Δ <i>envZ</i>	AE17 <i>envZ</i> -deletion mutant strain	This study
AE17C- <i>envZ</i>	Cm ^r , AE17Δ <i>envZ</i> with the complement plasmid pSTV28- <i>envZ</i>	This study
Plasmids		
pKD46	Amp ^r , expresses λ red recombinase, temperature-sensitive	Takara
pKD3	Amp ^r Cm ^r , <i>cat</i> gene, confers resistance to chloramphenicol template plasmid	Takara
pCP20	Amp ^r Cm ^r , temperature-sensitive plasmid	Takara
pSTV28	Cm ^r , cloning vector with pACYC184 replication starting point	Takara
pSTV28- <i>envZ</i>	Cm ^r , pSTV28 with <i>envZ</i> gene	This study

Abbreviations: Cm^r, chloramphenicol-resistant; Amp^r, ampicillin-resistant; APEC, Avian pathogenic *E. coli*.

techniques (Datsenko and Wanner, 2000). The primers used are listed in Table 2. Briefly, AE17 genomic DNA was used to amplify *envZ* upstream and downstream segments using *envZ*-up-F/R and *envZ*-down-F/R primers, respectively. The pKD3 plasmid was used to amplify a chloramphenicol resistance fragment with *envZ*-cm-F/R primers. Using the overlap PCR method and *envZ*-up-F and *envZ*-down-R primers, the 3 fragments (as templates) were used to amplify a fragment of *envZ* containing the chloramphenicol (Cm) resistance fragment. The fragment was then electroporated (200 Ω and 2,500 V) using a Gene Pulser MX cell (Bio-Rad, Hercules, CA) into AE17 competent cells containing the pKD46 plasmid. Then, the pCP20 plasmid was transformed into mutant strain AE17Δ*envZ* cells to delete the Cm cassette. Finally, the mutant strain was identified using *envZ*-out-F/R and *envZ*-in-F/R primers and named AE17Δ*envZ*.

For the complemented strain, the *envZ* fragment from AE17 was amplified using *envZ*-BamHI-F/*envZ*-PstI-R primers. The pSTV28 plasmid and *envZ* fragment were digested with restriction endonucleases BamHI and PstI (TaKaRa, Dalian, Liaoning, China) at 37°C for 1 h, ligated with T4 ligase (TaKaRa) at 4°C for 12 h, and transformed into *E. coli* DH5α cells (TaKaRa). The recombinant plasmid pSTV28-*envZ*-DH5α was constructed and electroporated into AE17Δ*envZ* cells, confirmed using *envZ*-BamHI-F/*envZ*-PstI-R primers, and named AE17C-*envZ*.

Growth Curves

Growth curves of AE17, AE17Δ*envZ*, and AE17C-*envZ* were monitored as described previously (Fu et al., 2022). Briefly, all 3 strains were cultured to the logarithmic growth phase and transferred into LB medium at a 1:100 volume ratio. The cell density was monitored hourly using a spectrophotometer (Bio-Rad), and the growth curves of strains were plotted.

Table 2. Primers used in this study.

Primer name	Sequence (5'-3')	Size/bp
AE17-F	GAGCGATCTTGGCTATACC	1,023
AE17-R	GTGAAGCTATCTAACCAACGG	
<i>envZ</i> -up-F	GCGGGCCACGCAACGAAAGTTAT	810
<i>envZ</i> -up-R	CCAGCCTACAACCATTAGCGGCACGGGATTAGGGC	
<i>envZ</i> -cm-F	CGCTAATGGTTGTAGGCTGGAGCTGCTT	1,033
<i>envZ</i> -cm-R	TGAACCTTCGCCATATGAATATCCTCCTTAG	
<i>envZ</i> -down-F	TATTCATATGGCGAAGTTCAGCACACCAGATA	736
<i>envZ</i> -down-R	CGAAGCGTCGCTAATGCAGAACA	
<i>envZ</i> -in-F	TCCCGTCATAGCCACTT	499
<i>envZ</i> -in-R	TTCATCAGGGCGATTCTC	
<i>envZ</i> -out-F	ATCAAACCCAGTACCACTTCTCT	2,102
<i>envZ</i> -out-R	GCTCTCCCGCGATAAGCT	
<i>envZ-BamHI</i> -F	CGCGGATCC ATGAGGCGATTGCGCTTCTC	1,353
<i>envZ-PstI</i> -R	AA ACTGCA GTACCCTTCTTTTGTTCATGC	
pKD46-F	CATACCGTCCGTTCTTTCTT	888
pKD46-R	TGATGATACCGCTGCCTTACT	
pCP20-F	TTAGTGGTTGTAACAAACACCTGACC	409
pCP20-R	GTTAGCGTTGAAGAATTTAGCCC	
pKD3-F	TGTAGGCTGGAGCTGCTT	1,013
pKD3-R	CATATGAATATCCTCCTTAGTTC	
pSTV28-F	CAGGAAACAGCTATGAC	102
pSTV28-R	GTTTTCCAGTCACGAC	

Restriction sites are indicated by bolded and underlined nucleotides.

Biofilm Formation Assay

The ability of all 3 strains to generate biofilms was determined using crystal violet (CV) assays as described previously (Yu et al., 2020). The strains were separately cultured to a logarithmic growth phase, diluted in LB liquid medium at a 1:50 volume ratio, and added to the glass test tubes and 96-well polypropylene plates, with 3 replicates/group. Test tubes and plates were incubated at 28°C for 48 h and the supernatant was discarded. Biofilms were washed 3 times in PBS. After air-drying, 0.1% (w/v) crystal violet (Sangon) was added, biofilms stained for 20 min, and washed 3 times in PBS. After air-drying, 33% (w/v) acetic acid (Sangon) was added to wells to fully dissolve biofilms which were measured at OD_{492nm} using a MicroELISA auto reader (Thermo Scientific, Pittsburgh, PA).

Scanning Electron Microscopy

Bacterial biofilms were visualized by scanning electron microscopy (SEM) as described (Yin et al., 2019). Briefly, bacteria cultures were added to 6-well plates and incubated with crawls for 48 h at 28°C. Crawls were removed, washed 3 times in PBS, fixed in 2.5% (w/v) glutaraldehyde at 4°C for 2 h, washed in PBS, fixed in 3% (w/v) glutaraldehyde at 4°C for 6 h, and washed 3 times in PBS for 20 min. The crawls were treated with 30%, 50%, 70%, 80%, 95%, and 100% (w/v) anhydrous ethanol at 4°C for 20 min. Ethanol solutions were discarded and crawls were treated in acetone at 4°C for 20 min. Then, crawls were freeze-dried using a Critical Point Drier (Emitech, Ashford, UK) and microscopic biofilm morphology was observed using a Hitachi S-4800 SEM (Hitachi, Tokyo, Japan).

Rdar Colony Morphotype Assay

Bacterial rdar morphotype was performed as described previously (Li et al., 2019). Briefly, all strains were cultured in LB medium to logarithmic growth phase, centrifuged at 5,000 × *g* for 10 min at 4°C, and washed twice in PBS to adjust the OD_{600nm} to 3.0. Then, 2 μL of each culture was plated onto a Congo red agar plate and incubated at 28°C for 3 d. Recipe for Congo Red medium: 10 g peptone, 5 g yeast powder, 8 g agar powder, 0.04 g Congo Red (Sangon) and 0.02 g Comas Brilliant Blue (Sangon), dissolved in 1 L of water.

Bacterial Resistance to Environmental Stress Assay

The resistance to diverse environmental stress assay was determined as described (Han et al., 2014). Briefly, strains were cultured to logarithmic phase, centrifuged at 5,000 × *g*, washed twice in PBS, and cells resuspended in an equal volume of PBS. For the acid assay, 100 μL bacteria and 900 μL LB medium (pH 3) were incubated at 37°C for 30 min; for the alkali assay, 100 μL bacteria and 900 μL Tris-HCl (100 mmol/L, pH 10) were incubated at 37°C for 30 min; for the oxidative stress assay, 100 μL bacterial and an equal volume of 10 mM hydrogen peroxide were incubated at 37°C for 1 h; and for the osmotic pressure assay, 100 μL bacteria and an equal volume of NaCl (4.8 mol/L) were incubated at 37°C for 1 h. Surviving bacteria were counted on agar plates using a 10-fold gradient dilution approach.

Serum Bactericidal Assay

The serum bactericidal assay was performed as described previously (Zhang et al., 2021). The 3 strains were cultured to the logarithmic growth phase,

centrifuged at $5,000 \times g$ for 10 min, washed 3 times and resuspended in PBS. Specific pathogen-free (SPF) chicken serum (Beyotime, Shanghai, China) was diluted with PBS to 0%, 12.5%, 25%, 50%, or 100%. Heat-inactivated serum was used as a negative control. Then, a 10 μ L bacterial culture was inoculated into 190 μ L of different serum concentrations, mixed, and incubated at 37°C for 30 min. Cultures were diluted in a 10-fold gradient, inoculated onto LB plates, incubated and counted for the number of surviving bacteria.

Bacterial Adherence Assay

The bacterial adherence assay was performed as described previously (Tu et al., 2021). The 3 strains were grown to a logarithmic phase, centrifuged, washed in PBS, and resuspended with Dulbecco's modified Eagle's medium (DMEM) (Biological Industries, Kibbutz Beit Haemek, Israel). Chicken embryonic fibroblast DF-1 cells were co-cultured with bacteria for 1.5 h at 37°C under 5% CO₂ according to a multiplicity of infection (MOI) of 100, and the cells were washed 3 times with PBS to remove the nonadherent bacteria and cells were lysed in 0.5% TritonX-100 (Beyotime). Lysates were diluted in a 10-fold gradient to count bacteria on LB agar plates.

Chick Infections

The Institutional Animal Care and Use Committee (IACUC) guidelines of Anhui Agricultural University (Number: 2021-021) were followed during chicken studies. One-day-old Romany broiler chicks were purchased from Anhui Anqin Poultry Company Ltd. (Anhui Province, Hefei, China). The chicks live in a clean and tidy environment at around 35°C and can freely eat food and drink water. There were 8 chicks in each group. The strains were cultured to the logarithmic growth phase (10^8 colony forming units (CFU)/mL), washed with PBS, and diluted to 10^5 CFU/mL (Yi et al., 2019; Fu et al., 2022). After a week of feeding, the chicks were injected intramuscularly into the legs with 10^5 CFUs of the bacterial solution, and negative controls were injected with an equal volume of PBS. Chick morbidity and mortality were observed daily for 7 d, and a survival curve was drawn to compare strain virulence.

To determine the effect of *envZ* on APEC colonization in vivo, the systemic infection experiment of the chick model was conducted as described previously (Zhang et al., 2021). Briefly, the wild-type strain AE17 and mutant strain AE17 Δ *envZ* and complemented strain AE17C-*envZ* were cultured to the logarithmic growth phase, washed and resuspended in PBS. Romany chickens were infected intramuscularly with a bacterial suspension containing 10^6 CFUs and euthanized humanely at 24 h postinfection. And chickens were euthanized, dissected, and disinfected with alcohol on the surface of the organs, scissors and forceps were overcooked and the heart, liver, spleen, and lung were collected under aseptic conditions, weighed and

homogenized. Serial dilutions of the homogenates were plated onto LB plates to count the bacterial numbers, and the ability of these APEC strains to colonize the liver, spleen, and blood was compared.

Library Preparation and Transcriptome Sequencing

RNA sequencing and library construction were performed at the Novogene Co., Ltd, Shenzhen, China. Total RNA was extracted from AE17 and AE17 Δ *envZ* strains using the RNeasy Mini Kit (Qiagen, Hilden, Germany) according to the manufacturer's instructions and RNA integrity was assessed using the RNA Nano 6000 Assay Kit of the Bioanalyzer 2100 system (Agilent Technologies, Santa Clara, CA). A total amount of 3 μ g RNA per sample was used as input material for the RNA sample preparations. Sequencing libraries were generated using NEBNext Ultra Directional RNA Library Prep Kit for Illumina (NEB, Ipswich, MA), and index codes were added to attribute sequences to samples. Library fragments were purified with AMPure XP system (Beckman Coulter, Brea, CA) and library quality was assessed on the Agilent Bioanalyzer 2100 system (Agilent, Santa Clara, CA). Library preparations were sequenced on the Illumina HiSeq platform (Illumina, San Diego, CA) and paired-end reads were generated. The raw data (raw reads) of fastq format are removed from reads containing adapter, reads containing ploy-N and low-quality reads to obtain clean data (clean reads). All downstream analyses are performed based on high-quality clean data. Sequence reads were mapped onto *E. coli* APEC O2-211 complete genome (NZ_CP006834.2) and filtered sequences were analyzed using Bowtie2-2.2.3 (Langmead et al., 2009). The number of reads mapped to each gene was counted with HTSeq v0.6.1 (Trapnell et al., 2009). The reads per kb of fragments per kilobase of exon per million fragments (FPKM) for each gene were calculated based on the length of the gene and reads count mapped to this gene. Differential expression analysis was performed using the DESeq R package (Nadler et al., 1997). Genes with an adjusted *P* value <0.05 identified by DESeq were assigned as differentially expressed genes (DEGs). Gene ontology (GO) enrichment analysis of DEGs was performed using the Goseq R package. We used KOBAS software to test for the statistical enrichment of DEGs in Kyoto Encyclopedia of Genes and Genomes (KEGG) pathways (Mao et al., 2005). Transcriptome sequencing reads were deposited at the National Center for Biotechnology Information gene expression database (<https://www.ncbi.nlm.nih.gov>) under the Sequence Read Archive (SRA) accession number: SUB94498265.

Quantitative Real-Time Reverse Transcription PCR

Quantitative real-time reverse transcription PCR (RT-qPCR) was used to assess the regulatory role of

Table 3. qRT-PCR primers used in this study.

Primer name	Sequence (5'-3')	Size/bp
<i>dnaE</i> -F	ATGTCGGAGGCGTAAGGCT	181
<i>dnaE</i> -R	TCCAGGGCGTCAGTAAACAA	
<i>ompC</i> -F	GAGGTTGTTAGCGTCGTATT	159
<i>ompC</i> -R	TTGGCGGCATCTATCACTT	
<i>ompT</i> -F	AGCCAGCAGCCACGATAGA	115
<i>ompT</i> -R	GAAGAAGGAGGCCGAAAAGTC	
<i>mlrA</i> -F	ATTACCCCGCCAGACACT	140
<i>mlrA</i> -R	CGAAGCCAGGCAAATAGAGA	
<i>mcbR</i> -F	GGCAGTTACTCTGGCTGTT	104
<i>mcbR</i> -R	GTTCCATGTCGCCCTTT	
<i>adiY</i> -F	AATATGAGCAACCAAAGTGT	118
<i>adiY</i> -R	GATAAGGGTGAATGGGAAAG	
<i>hdeB</i> -F	CTGGTGTCAATGCTTTTGGGA	134
<i>hdeB</i> -R	AGCGTTTATTTTTATGGGCG	
<i>hdeA</i> -F	GCCTGAACGATAGCTGGGGT	136
<i>hdeA</i> -R	ATTTCTGGCTGTGGACGAA	
<i>uspB</i> -F	GACCACCACAGACCACACA	157
<i>uspB</i> -R	TACCTCACATGGCCAACCC	
β - <i>actin</i> -F	TGAACTCCCTGATGGTCAGGTC	100
β - <i>actin</i> -R	ACCACAGGACTCCATACCCAAG	
<i>IL-1β</i> -F	CAATAAAATACCTCCACCCCG	106
<i>IL-1β</i> -R	ATGTTTCATTACCGTCCCGT	
<i>IL6</i> -F	AGACTTTACTCTCGTTTATGG	166
<i>IL6</i> -R	ATTGTTACTCTCTGGTTCTT	
<i>IL8</i> -F	CATCCACCTAAATCCATTCAAG	141
<i>IL8</i> -R	GGCATAAGTGCCTTTACGATC	

envZ in APEC on gene expression, including biofilm formation (*ompC*, *ompT*, *mlrA*, and *basR*) and stress response genes (*hdeA*, *hdeB*, *adiY*, and *uspB*). Additionally, to further analyze the mRNA levels of inflammatory cytokines (interleukin-1 β (IL-1 β), IL6, and IL8), DF-1 cells were infected with AE17, AE17 $\Delta envZ$, and AE17C-*envZ* strains. The gene primers are listed in Table 3. Transcription levels were normalized to the housekeeping genes *dnaE* and β -*actin*. Total RNA was extracted using the EasyPure RNA kit (TransGen, Beijing, China) and reverse transcribed to cDNA using the

EasyScript One-Step gDNA Removal and cDNA Synthesis SuperMix kit (TransGen) according to the manufacturer's instructions. cDNA was performed under the following conditions: 25°C for 10 min, 42°C for 15 min, and 85°C for 5 s. The RT-qPCR was performed using the TransStart Tip Green qPCR SuperMix kit (TransGen) on a 7500 Real-Time PCR System (Applied Biosystems, Foster City, CA). RT-qPCR was performed under the following conditions: 94°C for 30 s; 40 cycles at 94°C for 5 s, at 60°C for 15 s, and at 72°C for 10 s; and 94°C for 15 s, 60°C for 60 s, and 94°C for 15 s. The specific amplification of each gene was confirmed using melting curve analysis and the relative fold change was calculated using the $2^{-\Delta\Delta Ct}$ method (Livak and Schmittgen, 2001).

Statistical Analyses

These assay data were analyzed in GraphPad Prism 7.0 software package (GraphPad Software, LaJolla, CA). Statistical comparisons between groups were made using paired *t* tests. Two-way ANOVA was used to analyze RT-qPCR results. A *P* < 0.05 value was considered statistically significant.

RESULTS

EnvZ Did Not Affect APEC Growth

The mutant AE17 $\Delta envZ$ and the complemented strain AE17C-*envZ* were successfully constructed using λ -red recombination techniques (Figures 1A and 1B). AE17, AE17 $\Delta envZ$, and AE17C-*envZ* growth curves showed no significant differences, suggesting *EnvZ* did not affect APEC growth (Figure 1C).

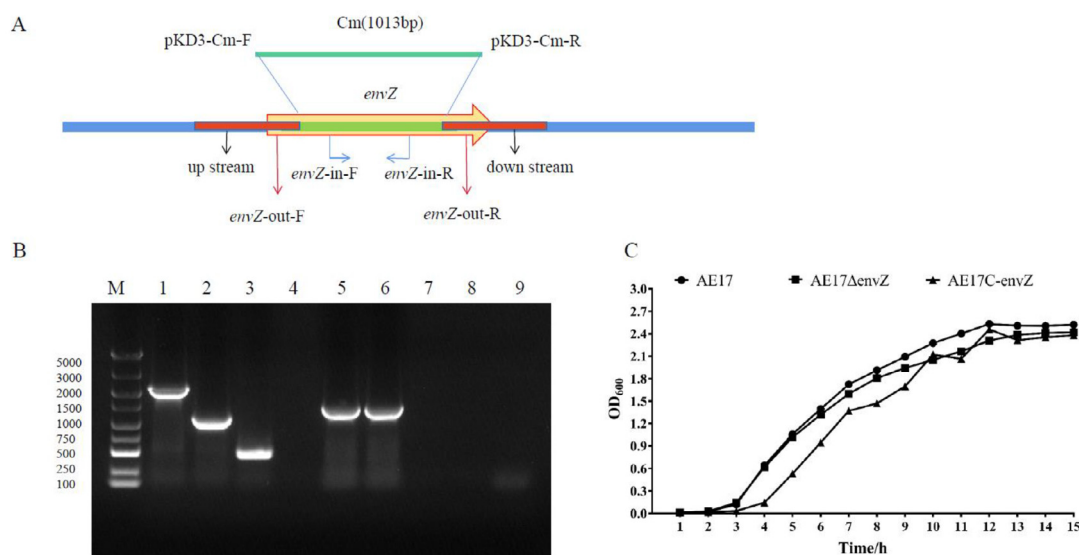


Figure 1. Identification and characteristics of the *envZ* gene mutant and complemented strains. (A) The schematic diagram of the strategy for deleting the *envZ* gene in AE17; (B) confirmation of the mutant strain AE17 $\Delta envZ$ and the complemented strain AE17C-*envZ*. M: 5000 DNA marker; Lane 1: PCR product (2012 bp) amplified from AE17 with primers *envZ*-out-F/R; Lane 2: PCR product (976 bp) amplified from AE17 $\Delta envZ$ with primers *envZ*-out-F/R; Lane 3 and 5: PCR product (499 bp) amplified from AE17 with primers *envZ*-in-F/R; Lane 4: PCR product (0 bp) amplified from AE17 $\Delta envZ$ with primers *envZ*-in-F/R; Lane 6: PCR product (499 bp) amplified from AE17C-*envZ* with primers *envZ*-in-F/R; Lane 7–9: negative control. (C) Growth curves of AE17, AE17 $\Delta envZ$, and AE17C-*envZ* strains in LB medium at 37°C, and the OD_{600nm} was measured every hour. The mutant strain shows a similar growth rate with the wild-type and complemented strains.

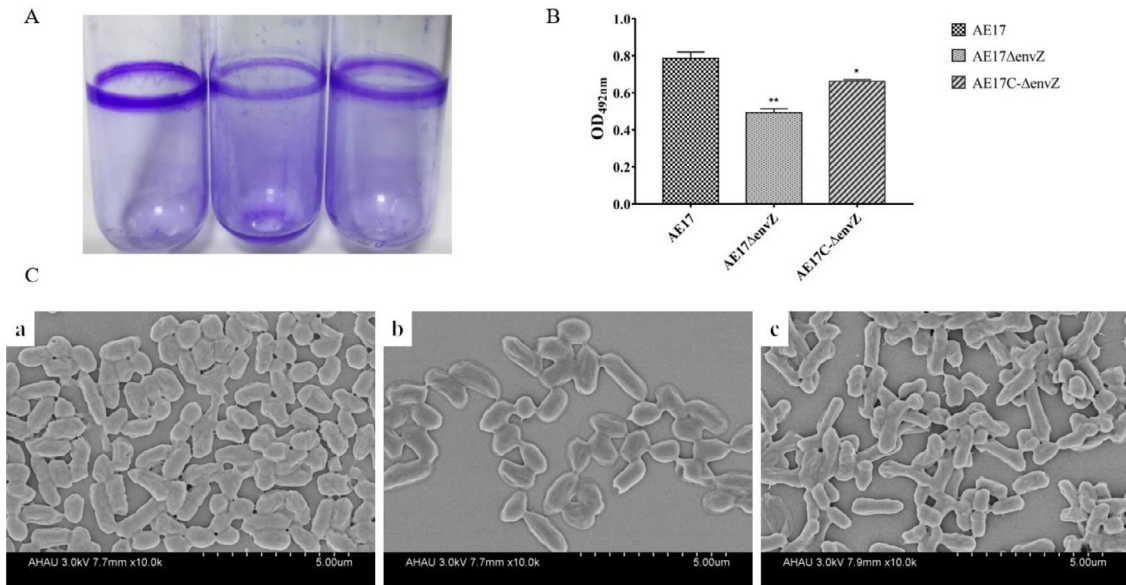


Figure 2. The ability of 3 strains to form biofilms was tested by crystal violet (CV) and scanning electron microscope (SEM) assays. (A, B) Analyze the biofilms ability of AE17, AE17Δ*envZ*, and AE17C-*envZ* strains using CV assay (* $P < 0.05$, ** $P < 0.01$). The biofilm formation of the mutant strain AE17Δ*envZ* was reduced compared with the wild-type strain. (C) (a) The morphological observation of AE17 ($\times 10,000$); (b) the morphological observation of AE17Δ*envZ* ($\times 10,000$); (c) the morphological observation of AE17C-*envZ* ($\times 10,000$).

Deletion of the EnvZ Gene Down-Regulated APEC Biofilm Formation

The biofilm formation abilities were determined using CV and SEM assays. AE17Δ*envZ* biofilm formation was significantly lower when compared with the AE17 strain, whereas the complemented strain AE17C-*envZ* was restored to a level similar to that of the wild-type strain (Figures 2A and 2B). SEM showed that AE17 biofilms were thicker with tight connections between bacteria, whereas AE17Δ*envZ* biofilms were thinner and connections were relatively loose, and complemented strain AE17C-*envZ* restored biofilm formation capacity (Figure 2C). These results indicate that EnvZ exerts a negative role in APEC biofilm formation.

EnvZ Influences the APEC Morphotype

We investigated the colony morphology of the 3 strains on Congo Red plates at 28°C for 3 d (Figure 3). The AE17 strain displayed a rdar morphotype

indicating curli and cellulose production. The *envZ* mutant strain displayed a saw (smooth and white) morphology, indicating a lack of both curli and cellulose production. The complemented AE17C-*envZ* strain also displayed a rdar morphology. These results suggested *envZ* deletion attenuated the APEC rdar morphotype.

Deletion of the EnvZ Gene Decreased APEC Environmental Stress Resistance

EnvZ functions as a histidine kinase to monitor and transduce osmolarity, so we evaluated its effects on an APEC strain's ability to adapt to different environments. Under acid, alkali, osmotic pressure, and oxidative stress conditions, when compared with the AE17, the survival rate of AE17Δ*envZ* was significantly reduced, whereas AE17C-*envZ* survival was restored to WT levels (Figure 4). Thus, EnvZ may help APEC strains adapt to extraintestinal environments and survive stressful conditions.

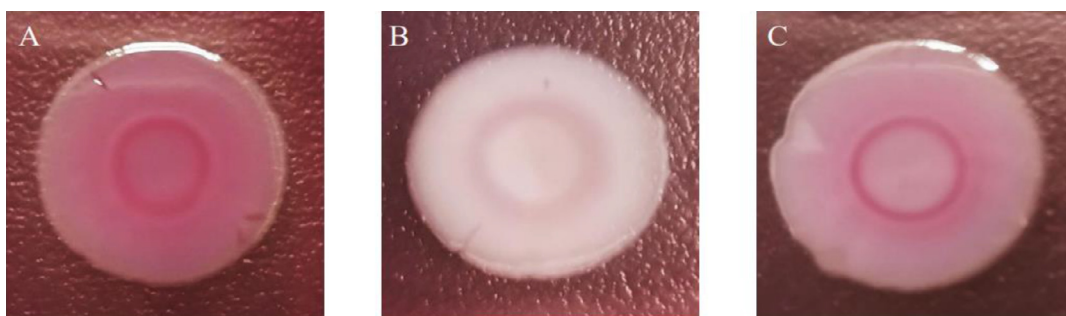


Figure 3. Bacterial display altered colony morphotypes. The AE17, AE17Δ*envZ*, and AE17C-*envZ* strains were investigated on Congo Red agar plate at 28°C for 3 d. (A) AE17 displays the rdar morphotype; (B) AE17Δ*envZ* results in the saw morphotype; (C) AE17C-*envZ* also displays the rdar morphotype.

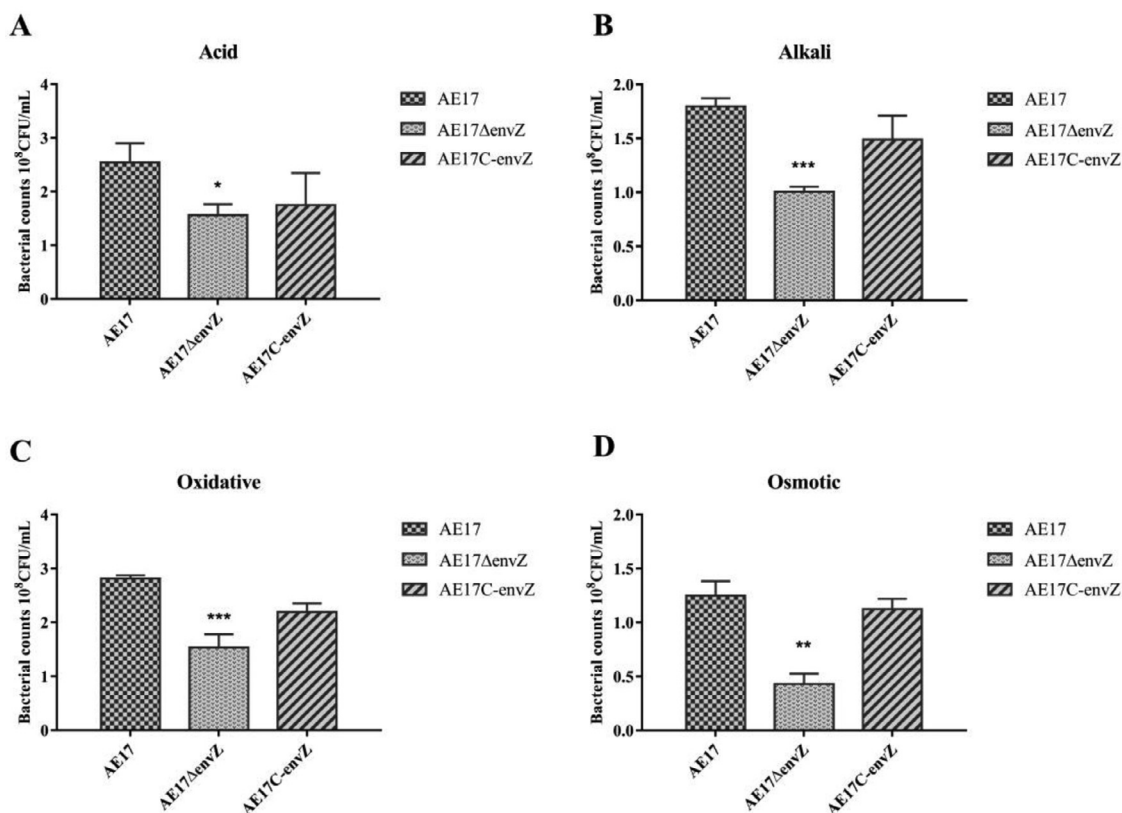


Figure 4. Bacterial resistance to environmental stress. The survival ability of AE17, AE17 $\Delta envZ$, and AE17C-*envZ* strains were tested under diverse environmental stress. (A) Acid (PH 3); (B) alkali (PH 10); (C) oxidative (10 μ M H₂O₂); and (D) osmotic (4.8 mol/L NaCl) (* P < 0.05, ** P < 0.01, and *** P < 0.001). Mutant strain shows decreased survival under diverse environmental stress conditions compared with wild-type and complemented strains.

Deletion of the EnvZ Gene Decreased Bacterial Serum Resistance

The AE17, AE17 $\Delta envZ$, and AE17C-*envZ* strains were separately incubated with serum at concentrations of 0%, 12.5%, 25%, 50%, or 100%. When compared with the wild-type AE17, the AE17 $\Delta envZ$ mutant strain was significantly susceptible to SPF chicken serum, whereas the AE17C-*envZ* strain survival was not restored (Figure 5). These results indicated EnvZ was involved in APEC's serum resistance.

EnvZ Influences Adherence and Inflammatory Responses Expression in DF-1 Cells

The role of *envZ* in bacterial adhesion was investigated by infecting DF-1 chicken fibroblast cells assay. The ability of AE17 $\Delta envZ$ to adhere to DF-1 cells was significantly enhanced when compared with the AE17, whereas the adherence to DF-1 cells of AE17C-*envZ* was lower compared with that of mutant strain and restored to a level to that of the wild-type strain (Figure 6A). These results indicate that EnvZ plays an important role in APEC adherence to DF-1 cells. And the relative expression levels of IL-1 β , IL-6, and IL-8 were

significantly increased in AE17 $\Delta envZ$ after infecting cells (Figure 6B).

Deletion of EnvZ Gene Attenuates APEC Virulence and Colonization In Vivo

To explore how *envZ* affected APEC virulence in vivo, we compared the pathogenicity of AE17, AE17 $\Delta envZ$, and AE17C-*envZ* strains in a 7-day-old chick systemic infection model. The mortality rate of the AE17 strain was 100% (8/8 chicks), AE17 $\Delta envZ$ strain was 62.5% (5/8 chicks), and AE17 C-*envZ* strain was 87.5% (7/8 chicks) (Figure 7A). Chicks infected with AE17 $\Delta envZ$ died later than those infected with AE17 and AE17C-*envZ*. The virulence of the mutant strain was attenuated compared to the wild-type and complemented strains. Thus, EnvZ was required for APEC virulence in vivo.

To further investigate whether *envZ* could influence APEC colonization during systemic infection, the number of bacteria in the heart, liver, spleen, and lung tissue of chicks was measured 24 h after postinfection. When inoculated intramuscularly, the amount of mutant strain was significantly reduced in the heart, liver, spleen, and lung compared to the wild-type strain. And the number of complement strains in these tissues recovered to levels similar to those of the wild-type strain

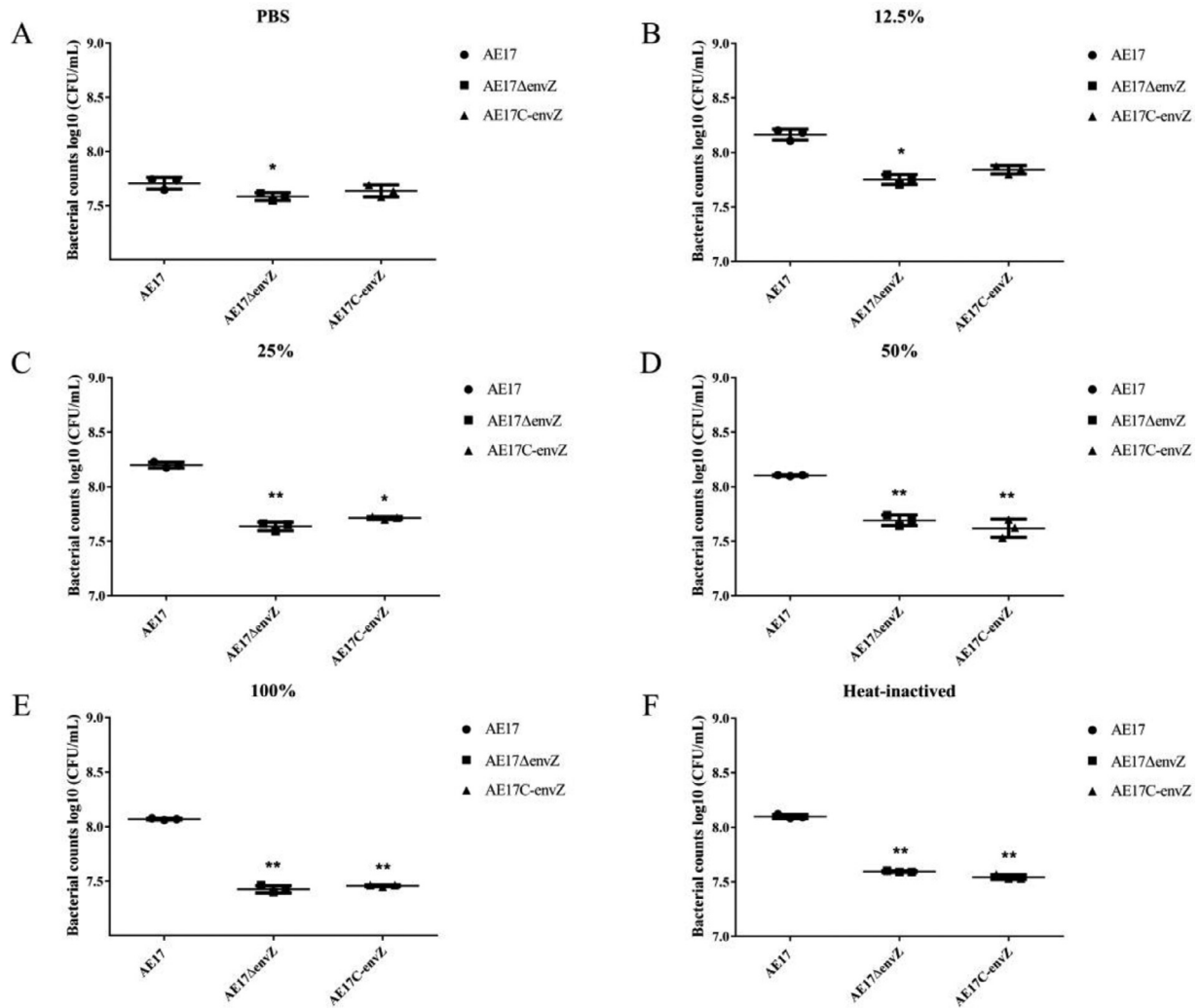


Figure 5. Serum bactericidal assay. SPF chicken serum at concentrations of 0%, 12.5%, 25%, 50%, 100%, and heat-inactivated. The AE17, AE17ΔenvZ, and AE17C-envZ strains were incubated with different dilutions of SPF chicken serum (* $P < 0.05$, ** $P < 0.01$). The mutant strain shows decreased survival in SPF chicken serum compared with the wild-type strain.

(Figure 7B). These results suggest that EnvZ is necessary for effective APEC colonization during systemic infection in vivo.

Identification of DEGs

To further understand how EnvZ contributed to APEC biological processes and pathogenicity, we compared gene transcript level changes in AE17 and envZ mutant strains by RNA-Seq. Clean reads from AE17 and AE17ΔenvZ were compared to the APEC O2-211 genome; the comparisons were 89.92% and 88.44%, respectively. According to the criteria of P value ≤ 0.05 , $|\log_2(\text{fold change})| \geq 1$, 711 DEGs were significantly regulated, of which 303 genes were significantly up-regulated and 408 genes were significantly down-regulated in the envZ mutant strain when compared to the AE17 (Figure 8A). These genes were mainly involved in biofilm formation, TCSs, Iron–Sulfur (Fe–S), phosphotransferase system (PTS), and bacterial flagella (Table 4).

In total, 269 DEGs were annotated in the GO database, and 1,163 GO functional annotations were

generated. DEGs were involved in 2 main GO categories: biological processes and molecular functions. Most DEGs participated in binding, ion binding, small molecule binding, biological regulation, and organic cyclic compound binding (Figure S1; Table S1). KEGG annotations identified 661 DEGs, involving 78 signaling pathways, including metabolic pathways, microbial metabolism in diverse environments, biosynthesis of amino acids, sulfur metabolism, TCSs, flagellar assembly, and biofilm formation (Figures 8B and S2; Table S2).

Deletion of EnvZ Gene Down-Regulated the Expression of Biofilms and Stress Response Genes

To validate RNA-Seq results, RT-qPCR studies were undertaken to examine the transcript levels of biofilm formation-associated genes (*ompC*, *ompT*, *mlrA*, and *basR*) and stress response genes (*hdeA*, *hdeB*, *adiY*, and *uspB*). OmpC, the pore protein of the outer membrane of *E. coli*, contributes to *Salmonella typhimurium* and APEC pathogenicity (Chatfield et al., 1991;

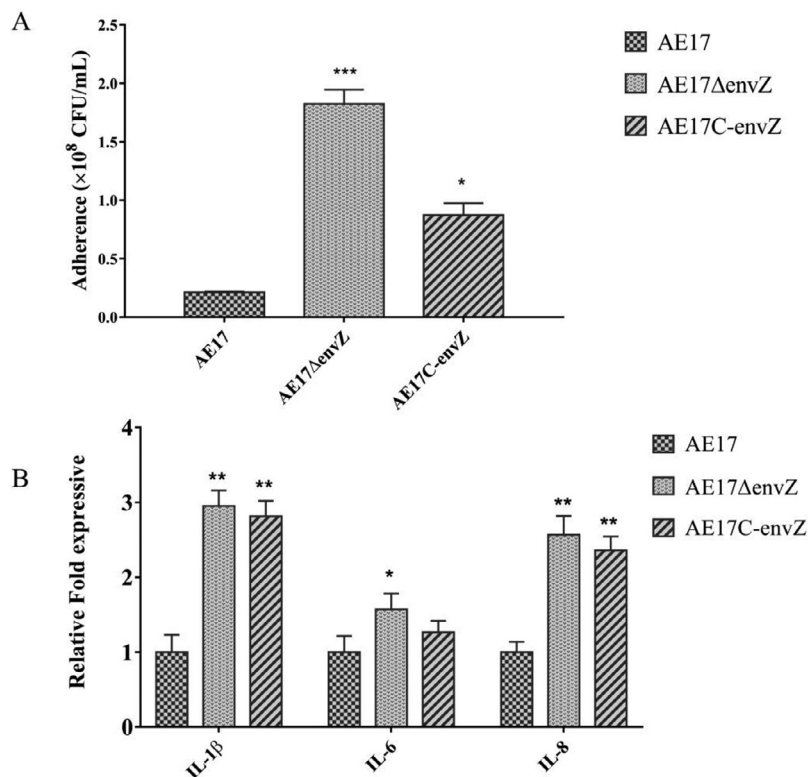


Figure 6. Bacterial adherence and inflammatory cytokines to DF-1 cells. (A) The DF-1 cells were infected with APEC strains for 1.5 h and the ability of AE17, AE17 Δ envZ, and AE17C-envZ strains to adhere to DF-1 cells was counted. (B) The relative expression levels of the inflammatory factors IL-1 β , IL-6, and IL-8 were tested by qRT-PCR (* $P < 0.05$, ** $P < 0.01$, *** $P < 0.001$).

Hejair et al., 2017b). Outer membrane protein OmpT is a protease in *E. coli* and plays important role in APEC pathogenicity (Hejair et al., 2017a). MlrA is a MerR family transcriptional regulator and a key regulator of biofilm formation (Ogasawara et al., 2010; Lindenberg et al., 2013). BasR is a RR of BasSR, with BasSR having roles in APEC biofilms and virulence (Yu et al., 2020). The *hdeA* and *hdeB* genes encode the acid-activated periplasmic chaperones HdeA and HdeB, respectively, to protect the *E. coli* periplasmic proteome against rapid acid-mediated damage to the mammalian stomach (Dahl et al., 2015). AdiY is an AraC family transcription regulator protein and regulates acid stress in some strains (Krin et al., 2010). The universal stress protein UspB is an integral membrane protein and is required for resistance to different starvation and stress conditions (Farewell et al., 1998). The transcript levels of these genes were significantly reduced in the AE17 Δ envZ strain when compared with the AE17 strain and were restored in the AE17C-envZ strain (Figure 9). Therefore, EnvZ executed a positive regulation on the expression of biofilms and stress response genes.

DISCUSSION

OmpR/EnvZ TCS is widely present in most Gram-negative or positive bacteria, detects and responds to extracellular osmolarity, and involves in bacterial pathogenesis, which can alter the expression of a variety of genes, including those encoding virulence factors,

antibiotic biosynthesis, motility, and biofilm formation (Bernardini et al., 1990; Xi et al., 2020). EnvZ is an HK of the OmpR/EnvZ TCS and has a key role in transducing osmotic signals in *E. coli* K12 (Gotoh et al., 2010; Cai et al., 2013; Breland et al., 2017) and contributes to *S. flexneri* and *V. cholerae* pathogenicity (Bernardini et al., 1990; Xi et al., 2020), but the role of its histidine kinase EnvZ in APEC's pathogenic process has not been reported. In this study, we demonstrated that EnvZ had central roles in APEC, including biofilm formation, rdar morphology, responses to environmental stresses, serum resistance, adhesion, immune system, and APEC virulence in vivo, suggesting that EnvZ has an important impact on the pathogenicity of APEC. And the transcriptome sequencing revealed that EnvZ is involved in metabolic pathways, microbial metabolism in diverse environments, biosynthesis of amino acids, sulfur metabolism, TCSs, flagellar assembly, and biofilm formation.

In this study, EnvZ was also involved in the response to various external environmental changes in APEC. In the process of infecting the host, bacteria will encounter some extreme environments, especially strong acids, strong alkalis, high osmolarity, oxidative stress, etc. Some genes have been reported to be critical for APEC's resistance to environmental stress, such as *ibeR*, *ybjX*, and *mcbR* (Wang et al., 2015; Yu et al., 2019; Song et al., 2020). Understanding the resistance of bacteria to environmental stress helps further explore the mechanisms of bacterial survival and infection. In *E. coli* K12, EnvZ interacts with the inner membrane

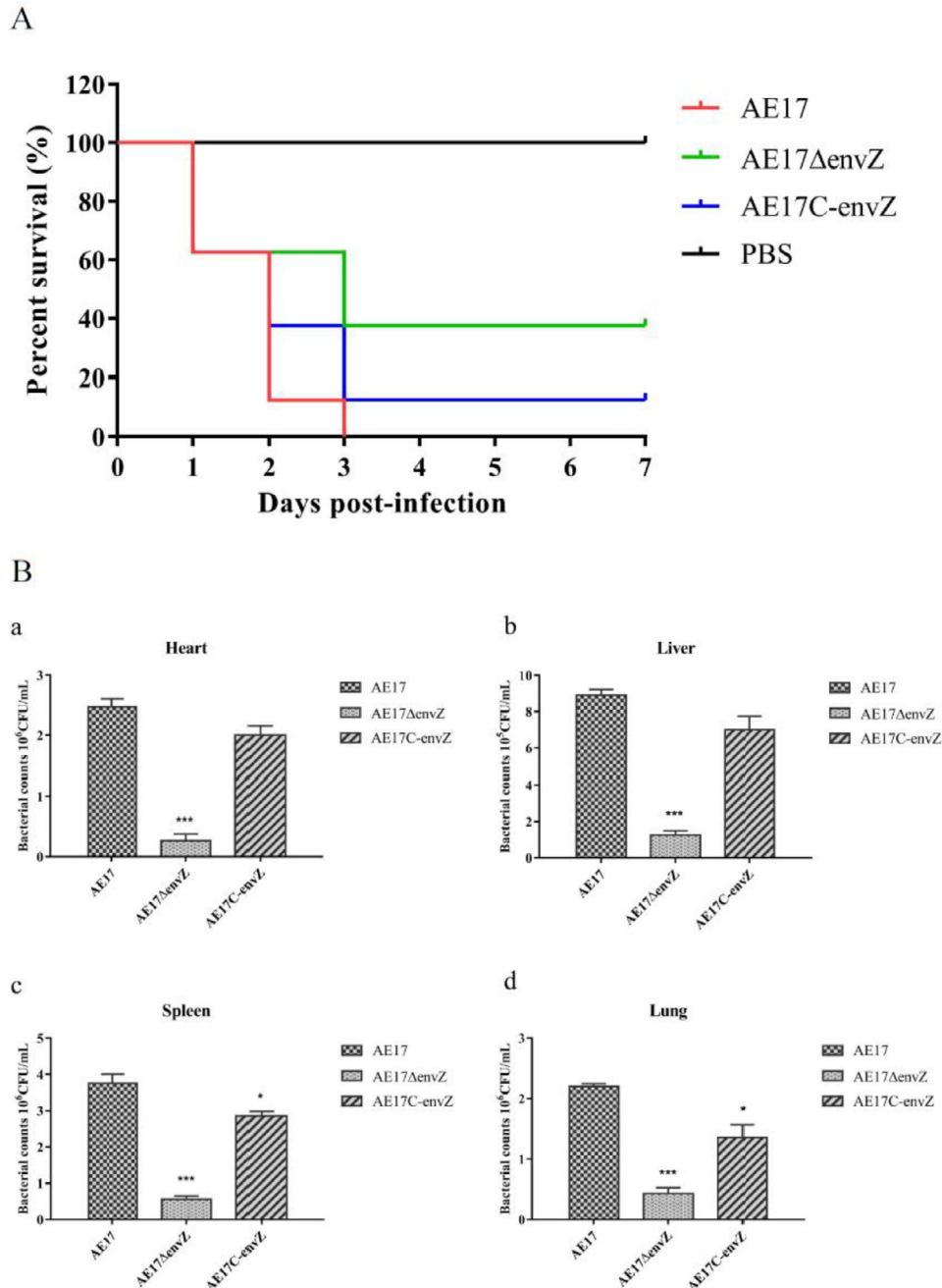


Figure 7. EnvZ is required for the virulence and colonization of APEC during systemic infection. (A) Determination of bacterial virulence. Seven-day-old chickens were injected intramuscularly with AE17, AE17 Δ envZ and AE17C-envZ at 10^5 CFU. Negative controls were injected with PBS. Survival was monitored until 7 d postinfection. (B) Colonization of APEC strains in chickens during systemic infection. Seven-day-old chickens were infected intramuscularly with 10^6 CFU of each APEC strain. After 24 h postinfection, the mutant strain had significantly lower bacterial loads in the heart, liver, spleen, and lung compared to the wild-type and complemented strains. A nonparametric Mann–Whitney U test was conducted to determine statistical significance (* $P < 0.05$, ** $P < 0.01$).

protein MzrA and responds to environmental signals (Gerken et al., 2009). In this study, transcriptome sequencing data showed EnvZ also regulated the transcript levels of outer membrane protein genes, such as *ompC* and *ompT*. Moreover, transcriptome data also showed that EnvZ regulated the expression levels of stress-resistance genes, such as *hdeA* and *hdeB*. HdeA and HdeB are reported to involve in the acid stress response in *E. coli* and protect the *E. coli* periplasmic proteome against rapid acid-mediated damage to the mammalian stomach (Dahl et al., 2015). Together, these

results suggest that *envZ* decreased the resistance to environmental stress by the down-regulation of outer membrane proteins and stress response genes.

Biofilm formation is a common phenomenon in APEC infection with hosts, which facilitates resistance to antibiotics and disrupts host cell immune mechanisms to achieve sustained colonization in the host, so biofilms often cause chronic diseases (Skyberg et al., 2007). Many TCSs and their components contribute to APEC biofilm formation, such as PhoP/Q, CpxA, and OmpR (Matter et al., 2018; Yin et al., 2019; Fu et al., 2022). In

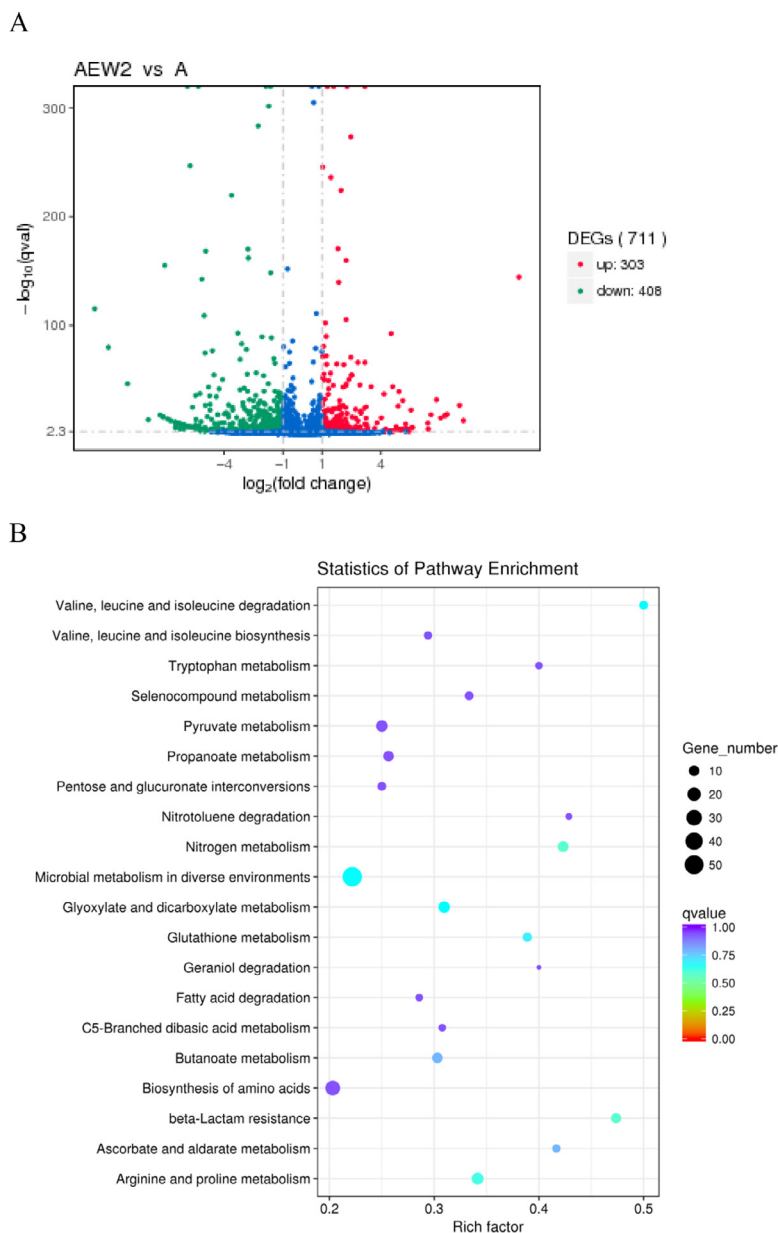


Figure 8. (A) Differential gene volcano plots. Volcano plots generated by EdgeR showing transcript expression profile in the comparison performed: AE17 $\Delta envZ$ and AE17 (AEW2 vs A). Significantly differentially expressed genes (DEGs) were defined as those with at least $|\log_2(\text{Fold-Change})| \geq 1$ (level of magnitude, vertical lines) and $q\text{-value} \leq 0.05$ (level of statistical significance, horizontal line). DEGs were illustrated in red (increased expression), green (decreased expression), and blue (not significant). (B) KEGG pathway classification analysis of DEGs. KOBAS software was used for KEGG pathway enrichment analyses. The abscissa shows the rich factor of DEGs and the ordinate indicates the top 20 of KEGG pathway enrichment for DEGs.

this study, deletion of the histidine kinase *envZ* gene reduced biofilm formation, and also weakened curli and cellulose production in APEC. It is worth noting that curli fimbriae have important roles in early biofilm formation stages (Prigent-Combaret et al., 2000; Ogasawara et al., 2010). And the transcriptome sequencing showed that EnvZ affects the biofilm formation signaling pathway, and many biofilms and curli fimbriae-associated genes were down-regulated in the *envZ*-deficient mutant strain, including *ompC*, *ompT*, *mlrA*, and *basR*. In *E. coli* MG1665, the OmpR/EnvZ TCS was shown to affect curli production (Prigent-Combaret et al., 2001; Jubelin et al., 2005). MerR family transcriptional regulator MlrA contributes to biofilm formation and interacts with *ydaM* to regulate the

expression of the curli fimbriae regulator CsgD in *E. coli* K12 (Ogasawara et al., 2010; Kojima and Nikaido, 2014). Our study supports that the biofilm formation and the production of curli fimbriae connect, but the regulation mechanism of EnvZ requires further study.

Innate immunity is the first line of defense against infection and tissue damage. Pattern recognition receptors, such as Toll-like receptors, recognize pathogens such as bacteria, trigger an immune response and activate intracellular signaling pathways leading to antimicrobial activity and the production of inflammatory cytokines, triggering a range of inflammatory responses (Ciornei et al., 2010; Wu et al., 2018; Chambers and Scheck, 2020). In *Yersinia pestis*, the OmpR/EnvZ TCS participates in the host's innate immune processes

Table 4. Partial differentially expressed genes (DEGs) in the *envZ*-deficient mutant strain.

Classification	Gene ID	Gene	Description	log ₂ ^{FC}	
TCS	b2370	<i>evgS</i>	Two-component system, NarL family, sensor histidine kinase EvgS	1.85	
	b2369	<i>evgA</i>	Two-component system, NarL family, response regulator EvgA	1.61	
	b4113	<i>basR</i>	BasR/S two-component system, OmpR family, response regulator BasR	-5.18	
Stress response	b1235	<i>rssB</i>	Two-component system, response regulator RssB	-1.27	
	b1296	<i>yecF</i>	Predicted amino acid transporter	-4.76	
	b3494	<i>uspB</i>	Universal stress protein UspB	-2.97	
	b1051	<i>msy</i>	Acidic protein MsyB	-2.8	
	b4116	<i>adiY</i>	AraC family transcription regulator protein AdiY, acid stress	-2.19	
	b3509	<i>hdeB</i>	Acid stress chaperone HdeB	-2.17	
Outer membrane	b3510	<i>hdeA</i>	Stress response protein; acid-resistance protein; acid stress chaperone HdeA	-1.29	
	b1024	<i>pgaA</i>	Biofilm PGA synthesis protein YcdS; predicted outer membrane protein	4.55	
	b1023	<i>ycdR</i>	Predicted enzyme associated with biofilm formation	4.45	
	b0488	<i>ybbJ</i>	Inner membrane protein	2.02	
	b2605	<i>yfiB</i>	Putative outer membrane lipoprotein	1.63	
	b0929	<i>ompF</i>	Outer membrane pore protein OmpF	1.59	
	b2215	<i>ompC</i>	Outer membrane porin protein OmpC	-5.3	
	b4149	<i>blc</i>	Outer membrane lipoprotein Blc precursor	-4.72	
	b4496	<i>nmpC</i>	Outer membrane porin protein NmpC	-3.82	
	b3522	<i>yhjD</i>	Membrane protein; conserved hypothetical protein	-3.01	
	b1285	<i>yciR</i>	c-di-GMP phosphodiesterase	-2.57	
	b2013	<i>yecE</i>	Inner membrane protein	-2.45	
	b3506	<i>slp</i>	Outer membrane lipoprotein	-2.21	
	b0565	<i>ompT</i>	Outer membrane protein 3b (a), protease VII	-2.16	
	b0112	<i>aroP</i>	Aromatic amino acid transport protein AroP	-1.96	
	b3688	<i>yidQ</i>	Outer membrane protein	-1.80	
	Fe-S cluster	b4291	<i>fecA</i>	Iron complex outer membrane receptor protein, putative iron compound receptor	7.37
b1451		<i>yncD</i>	Iron complex outer membrane receptor protein	3.24	
b1684		<i>sufA</i>	Fe-S cluster assembly protein SufA	-4.45	
b0150		<i>fhuA</i>	Iron complex outer membrane receptor protein; ferrichrome outer membrane transporter	-2.81	
b0150		<i>fhuA</i>	Iron complex outer membrane receptor protein	-2.81	
b1683		<i>sufB</i>	Fe-S cluster assembly protein SufB; component of SufBCD complex	-2.47	
b1682		<i>sufC</i>	Fe-S cluster assembly ATP-binding protein; component of SufBCD complex. ATP-binding component of ABC superfamily	-2.46	
b1681		<i>sufD</i>	Fe-S cluster scaffold complex subunit SufD	-2.28	
b1680		<i>sufS</i>	L-cysteine desulfurase	-1.84	
b2531		<i>iscR</i>	Rrf2 family transcriptional regulator, iron-sulfur cluster assembly transcription factor; DNA-binding transcriptional repressor	-1.19	
Flagellar		b1892	<i>flhD</i>	Flagellar transcriptional activator FlhD	-1.9
		b1891	<i>flhC</i>	Flagellar transcriptional activator FlhC	-1.3
		b1921	<i>fliZ</i>	Regulator of sigma S factor FliZ	-1.27
	b1940	<i>fliH</i>	Flagellar assembly protein FliH	-1.26	
	b1922	<i>fliA</i>	RNA polymerase sigma 28 (sigma F) factor for flagellar operon FliA	-1.19	
LPS	b0641	<i>rlpB</i>	LPS-assembly lipoprotein; minor lipoprotein	1.65	
	b0054	<i>imp</i>	LPS-assembly protein; organic solvent tolerance protein precursor	1.27	
	b3627	<i>rafI</i>	LPS alpha-1,3-glucosyl transferase	-6.72	
	b3626	<i>rfaJ</i>	Lipopolysaccharide 1,2-glucosyltransferase	-6.40	
	b3631	<i>rfaG</i>	Lipopolysaccharide core biosynthesis glucosyltransferase	-4.98	
	b3622	<i>waaL</i>	O-antigen ligase; lipid A-core, surface polymer ligase	-4.76	
	b3632	<i>rfaQ</i>	Lipopolysaccharide core biosynthesis glycosyltransferase	-4.59	
Drug resistance	b2685	<i>emrA</i>	Multidrug efflux pump membrane fusion protein EmrA	1.31	
	b2519	<i>pbpC</i>	Penicillin-binding protein	1.55	
	b3028	<i>mdaB</i>	The modulator of drug activity; NADPH quinone reductase	1.39	
	b4337	<i>mdtM</i>	Multidrug efflux pump/bile salt:H (+) antiporter/Na (+):H (+) antiporter/K (+):H (+) antiporter	-5.15	
	b0543	<i>emrE</i>	Multidrug/betaine/choline efflux transporter EmrE	-2.61	
PTS system	b2703	<i>srLE</i>	PTS system, glucitol/sorbitol-specific IIBC component	2.21	
	b3947	<i>ptsA</i>	Putative PTS multi-phosphoryl transfer protein PtsA	2.20	
	b2704	<i>srLB</i>	PTS system, glucitol/sorbitol-specific IIA component	2.00	
	b2702	<i>srLA</i>	PTS system, glucitol/sorbitol-specific IIC2 component	1.19	
	b2167	<i>fruA</i>	PTS system, fructose-specific IIBC component	-1.93	
	b1737	<i>celB</i>	PTS system, cellobiose-specific IIC component	-1.59	
	b3599	<i>mtlA</i>	Fused mannitol-specific PTS enzymes: IIA components/IIB components/IIC components	-1.61	
	b1738	<i>celA</i>	PTS system, cellobiose-specific IIB component; PEP-dependent phosphotransferase enzyme IV	-1.65	

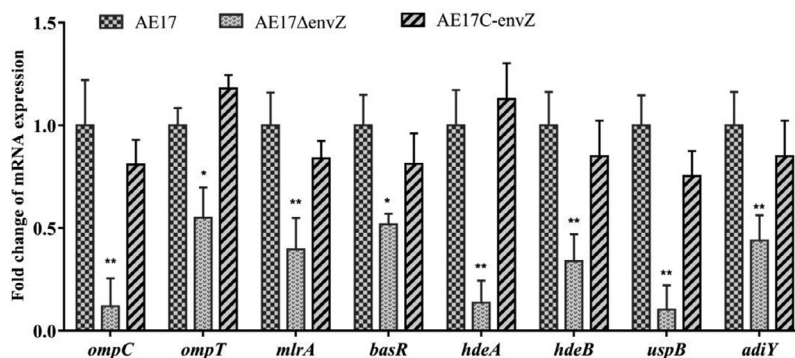


Figure 9. Relative expression of virulence genes was tested with qRT-PCR. These genes in the RNA-Seq results were selected for qRT-PCR verification. Data were normalized to the housekeeping gene *dnaE*. The X-axis represents different genes. The relative gene expression levels were calculated using the $2^{-\Delta\Delta C_t}$ method (** $P < 0.01$).

(Reboul et al., 2014). In this study, EnvZ is necessary for stimulating the host production of inflammatory cytokines during APEC systemic infection in vivo. In *S. flexneri*, the inactivation of *envZ* gene attenuated the invasion of the epithelial cell (Bernardini et al., 1990). In different bacteria, EnvZ exhibits different effects on host cell adhesion, suggesting that it may also regulate other key factors that still need to be further explored.

APEC is one of the main causes of bloodstream infection, which initially colonizes poultry via the respiratory tract and then spreads systemically (Dziva and Stevens, 2008). Serum resistance is an important virulence trait of APEC, and many bacterial traits contribute to *E. coli*'s serum resistance. It is indicated that many virulence factors contribute to the serum resistance of APEC, including the production of a capsule, a lipopolysaccharide (LPS) layer, and some outer membrane proteins (OMPs) (Li et al., 2011; Ma et al., 2018). In this study, we demonstrated that the inactivation of *envZ* led to more susceptibility to SPF chicken serum, which might be a reason for decreased expression of outer membrane genes due to *envZ* gene deletion. Studies have shown that the histidine kinase of TCS plays an importance in APEC virulence, including PhoQ, QseC, etc. (Chaudhari and Kariyawasam, 2014; Tu et al., 2016). Furthermore, EnvZ has also been required for *Acinetobacter baumannii* and *V. cholerae* virulence in some infection models (Tipton and Rather, 2017; Xi et al., 2020). In this study, the inactivation of *envZ* significantly attenuated APEC virulence in a chicken systemic infection model and decreased the bacterial colonization in the heart, liver, spleen, and lung tissues of chicks, indicating that EnvZ influences the bacterial survival and pathogenicity of APEC during systemic infection.

In conclusion, we demonstrated that EnvZ was essential for biological properties and virulence, including biofilm formation, curli production, stress responses, serum resistance, adhesion, and APEC pathogenicity. Transcriptomic studies showed EnvZ was involved in metabolic pathways, microbial metabolism in diverse environments, and biofilm formation. Generally, EnvZ mediates stress responses, and regulates and influences the expression and function of bacterial virulence factors involved in APEC pathogenesis.

ACKNOWLEDGMENTS

This work was supported by grants from the National Natural Science Foundation of China (grant no. 31772707, 31972644, 31802161), the University Synergy Innovation Program of Anhui Province (grant no. GXXT-2019-035).

DISCLOSURES

The authors declare that they have no known competing financial interests or personal relationships that could have appeared to influence the work reported in this paper.

SUPPLEMENTARY MATERIALS

Supplementary material associated with this article can be found in the online version at [doi:10.1016/j.psj.2022.102388](https://doi.org/10.1016/j.psj.2022.102388).

REFERENCES

- Bernardini, M. L., A. Fontaine, and P. J. Sansonetti. 1990. The two-component regulatory system OmpR-EnvZ controls the virulence of *Shigella flexneri*. *J. Bacteriol.* 172:6274–6281.
- Breland, E. J., A. R. Eberly, and M. Hadjifrangiskou. 2017. An overview of two-component signal transduction systems implicated in extra-intestinal pathogenic *E. coli* infections. *Front. Cell. Infect. Microbiol.* 7:1–14.
- Cai, W., Y. Wannemuehler, G. Dell'Anna, B. Nicholson, N. L. Barbieri, S. Kariyawasam, Y. Feng, C. M. Logue, L. K. Nolan, and G. Li. 2013. A novel two-component signaling system facilitates uropathogenic *Escherichia coli*'s ability to exploit abundant host metabolites. *PLoS Pathog.* 9:e1003428.
- Chambers, K. A., and R. A. Scheck. 2020. Bacterial virulence mediated by orthogonal post-translational modification. *Nat. Chem. Biol.* 16:1043–1051.
- Chatfield, S. N., C. J. Dorman, C. Hayward, and G. Dougan. 1991. Role of *ompR*-dependent genes in *Salmonella typhimurium* virulence: mutants deficient in both *ompC* and *ompF* are attenuated in vivo. *Infect. Immun.* 59:449–452.
- Chaudhari, A. A., and S. Kariyawasam. 2014. Innate immunity to recombinant QseC, a bacterial adrenergic receptor, may regulate expression of virulence genes of avian pathogenic *Escherichia coli*. *Vet. Microbiol.* 171:236–241.
- Ciornei, C. D., A. Novikov, C. Beloin, C. Fitting, M. Caroff, J. M. Ghigo, J. M. Cavillon, and M. Adib-Conquy. 2010. Biofilm-forming *Pseudomonas aeruginosa* bacteria undergo

- lipopolysaccharide structural modifications and induce enhanced inflammatory cytokine response in human monocytes. *Innate Immun.* 16:288–301.
- Dahl, J. U., P. Koldeewey, L. Salmon, S. Horowitz, J. C. A. Bardwell, and U. Jakob. 2015. HdeB functions as an acid-protective chaperone in bacteria. *J. Biol. Chem.* 290:65–75.
- Datsenko, K. A., and B. L. Wanner. 2000. One-step inactivation of chromosomal genes in *Escherichia coli* K-12 using PCR products. *Proc. Natl. Acad. Sci. U. S. A.* 97:6640–6645.
- Dziva, F., and M. P. Stevens. 2008. Colibacillosis in poultry: unravelling the molecular basis of virulence of avian pathogenic *Escherichia coli* in their natural hosts. *Avian Pathol.* 37:355–366.
- Farewell, A., K. Kvint, and T. Nyström. 1998. *uspB*, a new σ (S)-regulated gene in *Escherichia coli* which is required for stationary-phase resistance to ethanol. *J. Bacteriol.* 180:6140–6147.
- Fu, D., J. Wu, Y. Gu, Q. Li, Y. Shao, H. Feng, X. Song, J. Tu, and K. Qi. 2022. The response regulator OmpR contributes to the pathogenicity of avian pathogenic *Escherichia coli*. *Poult. Sci.* 101:101757.
- Gerken, H., E. S. Charlson, E. M. Cicirelli, L. J. Kenney, and R. Misra. 2009. MzrA: a novel modulator of the EnvZ/OmpR two-component regulon. *Mol. Microbiol.* 72:1408–1422.
- Gotoh, Y., Y. Eguchi, T. Watanabe, S. Okamoto, A. Doi, and R. Utsumi. 2010. Two-component signal transduction as potential drug targets in pathogenic bacteria. *Curr. Opin. Microbiol.* 13:232–239.
- Gushchin, I., I. Melnikov, V. Polovinkin, A. Ishchenko, A. Yuzhakova, P. Buslaev, G. Bourenkov, S. Grudinin, E. Round, T. Balandin, V. Borshchevskiy, D. Willbold, G. Leonard, G. Büldt, A. Popov, and V. Gordeliy. 2017. Mechanism of transmembrane signaling by sensor histidine kinases. *Science.* 356:1–12.
- Han, Y., X. Han, S. Wang, Q. Meng, Y. Zhang, C. Ding, and S. Yu. 2014. The *waaL* gene is involved in lipopolysaccharide synthesis and plays a role on the bacterial pathogenesis of avian pathogenic *Escherichia coli*. *Vet. Microbiol.* 172:486–491.
- Hejair, H. M. A., J. Ma, Y. Zhu, M. Sun, W. Dong, Y. Zhang, Z. Pan, W. Zhang, and H. Yao. 2017a. Role of outer membrane protein T in pathogenicity of avian pathogenic *Escherichia coli*. *Res. Vet. Sci.* 115:109–116.
- Hejair, H. M. A., Y. Zhu, J. Ma, Y. Zhang, Z. Pan, W. Zhang, and H. Yao. 2017b. Functional role of *ompF* and *ompC* porins in pathogenesis of avian pathogenic *Escherichia coli*. *Microb. Pathog.* 107:29–37.
- Herren, C. D., A. Mitra, S. K. Palaniyandi, A. Coleman, S. Elankumaran, and S. Mukhopadhyay. 2006. The BarA-UvrY two-component system regulates virulence in avian pathogenic *Escherichia coli* O78:K80:H9. *Infect. Immun.* 74:4900–4909.
- Jubelin, G., A. Vianney, C. Beloin, J. M. Ghigo, J. C. Lazzaroni, P. Lejeune, and C. Dorel. 2005. CpxR/OmpR interplay regulates curli gene expression in response to osmolarity in *Escherichia coli*. *J. Bacteriol.* 187:2038–2049.
- Kathayat, D., D. Lokesh, S. Ranjit, and G. Rajashekar. 2021. Avian pathogenic *Escherichia coli* (APEC): an overview of virulence and pathogenesis factors, zoonotic potential, and control strategies. *Pathogens.* 10:1–32.
- Khorchid, A., M. Inouye, and M. Ikura. 2005. Structural characterization of *Escherichia coli* sensor histidine kinase EnvZ: the periplasmic C-terminal core domain is critical for homodimerization. *Biochem. J.* 385:255–264.
- Kojima, S., and H. Nikaido. 2014. High salt concentrations increase permeability through ompc channels of *Escherichia coli*. *J. Biol. Chem.* 289:26464–26473.
- Krin, E., A. Danchin, and O. Soutourina. 2010. Decrypting the H-NS-dependent regulatory cascade of acid stress resistance in *Escherichia coli*. *BMC Microbiol.* 10:1–8.
- Langmead, B., C. Trapnell, M. Pop, and S. L. Salzberg. 2009. Ultrafast and memory-efficient alignment of short DNA sequences to the human genome. *Genome Biol.* 10:1–10.
- Li, F., A. Cimdins, M. Rohde, L. Jansch, V. Kaefer, M. Nimtz, and U. Römling. 2019. DncV synthesizes cyclic GMP-AMP and regulates biofilm formation and motility in *Escherichia coli* ECOR31. *MBio.* 10:1–21.
- Li, G., K. A. Tivendale, P. Liu, Y. Feng, Y. Wannemuehler, W. Cai, P. Mangiamale, T. J. Johnson, C. Constantinidou, C. W. Penn, and L. K. Nolan. 2011. Transcriptome analysis of avian pathogenic *Escherichia coli* O1 in chicken serum reveals adaptive responses to systemic infection. *Infect. Immun.* 79:1951–1960.
- Lindenberg, S., G. Klauck, C. Pesavento, E. Klauck, and R. Hengge. 2013. The EAL domain protein YciR acts as a trigger enzyme in a c-di-GMP signalling cascade in *E. coli* biofilm control. *EMBO J.* 32:2001–2014.
- Livak, K. J., and T. D. Schmittgen. 2001. Analysis of relative gene expression data using real-time quantitative PCR and the $2^{-\Delta\Delta CT}$ method. *Methods.* 25:402–408.
- Ma, J., C. An, F. Jiang, H. Yao, C. Logue, L. K. Nolan, and G. Li. 2018. Extraintestinal pathogenic *Escherichia coli* increase extracytoplasmic polysaccharide biosynthesis for serum resistance in response to bloodstream signals. *Mol. Microbiol.* 110:689–706.
- Mao, X., T. Cai, J. G. Olyarchuk, and L. Wei. 2005. Automated genome annotation and pathway identification using the KEGG Orthology (KO) as a controlled vocabulary. *Bioinformatics.* 21:3787–3793.
- Mascher, T., J. D. Helmann, and G. Uuden. 2006. Stimulus perception in bacterial signal-transducing histidine kinases. *Microbiol. Mol. Biol. Rev.* 70:910–938.
- Matter, L. B., M. A. Ares, J. Abundes-Gallegos, M. L. Cedillo, J. A. Yáñez, Y. Martínez-Laguna, M. A. De la Cruz, and J. A. Girón. 2018. The CpxRA stress response system regulates virulence features of avian pathogenic *Escherichia coli*. *Environ. Microbiol.* 20:3363–3377.
- Moulin-Schouleur, M., M. Répérant, S. Laurent, A. Brée, S. Mignon-Grasteau, P. Germon, D. Rasschaert, and C. Schouler. 2007. Extraintestinal pathogenic *Escherichia coli* strains of avian and human origin: link between phylogenetic relationships and common virulence patterns. *J. Clin. Microbiol.* 45:3366–3376.
- Nadler, S. G., D. Tritschler, O. K. Haffar, J. Blake, A. G. Bruce, and J. S. Cleaveland. 1997. Differential expression and sequence-specific interaction of karyopherin α with nuclear localization sequences. *J. Biol. Chem.* 272:4310–4315.
- Ogasawara, H., K. Yamamoto, and A. Ishihama. 2010. Regulatory role of MlrA in transcription activation of *csqD*, the master regulator of biofilm formation in *Escherichia coli*. *FEMS Microbiol. Lett.* 312:160–168.
- Oshima, T., H. Aiba, Y. Masuda, S. Kanaya, M. Sugiura, B. L. Wanner, H. Mori, and T. Mizuno. 2002. Transcriptome analysis of all two-component regulatory system mutants of *Escherichia coli* K-12. *Mol. Microbiol.* 46:281–291.
- Prigent-Combaret, C., E. Brombacher, O. Vidal, A. Ambert, P. Lejeune, P. Landini, and C. Dorel. 2001. Complex regulatory network controls initial adhesion and biofilm formation in *Escherichia coli* via regulation of the *csqD* gene. *J. Bacteriol.* 183:7213–7223.
- Prigent-Combaret, C., G. Prensier, T. T. Le Thi, O. Vidal, P. Lejeune, and C. Dorel. 2000. Developmental pathway for biofilm formation in curli-producing *Escherichia coli* strains: role of flagella, curli and colanic acid. *Environ. Microbiol.* 2:450–464.
- Reboul, A., N. Lemaître, M. Titecat, M. Merchez, G. Deloison, I. Ricard, E. Pradel, M. Marceau, and F. Sebbane. 2014. *Yersinia pestis* requires the 2-component regulatory system OmpR-EnvZ to resist innate immunity during the early and late stages of plague. *J. Infect. Dis.* 210:1367–1375.
- Skyberg, J. A., K. E. Siek, C. Doetkott, and L. K. Nolan. 2007. Biofilm formation by avian *Escherichia coli* in relation to media, source and phylogeny. *J. Appl. Microbiol.* 102:548–554.
- Song, X., M. Qiu, H. Jiang, M. Xue, J. Hu, H. Liu, X. Zhou, J. Tu, and K. Qi. 2020. *ybjX* mutation regulated avian pathogenic *Escherichia coli* pathogenicity through stress-resistance pathway. *Avian Pathol.* 49:144–152.
- Tipton, K. A., and P. N. Rather. 2017. An ompR-envZ two-component system ortholog regulates phase variation, osmotic tolerance, motility, and virulence in *Acinetobacter baumannii* strain AB5075. *J. Bacteriol.* 199:1–16.
- Tiwari, S., S. B. Jamal, S. S. Hassan, P. V. S. D. Carvalho, S. Almeida, D. Barh, P. Ghosh, A. Silva, T. L. P. Castro, and V. Azevedo. 2017. Two-component signal transduction systems of pathogenic bacteria as targets for antimicrobial therapy: an overview. *Front. Microbiol.* 8:1–7.
- Tokishita, S. I., A. Kojima, H. Aiba, and T. Mizuno. 1991. Transmembrane signal transduction and osmoregulation in *Escherichia*

- coli*: functional importance of the periplasmic domain of the membrane-located protein kinase. *EnvZ*. *J. Biol. Chem.* 266:6780–6785.
- Trapnell, C., L. Pachter, and S. L. Salzberg. 2009. TopHat: discovering splice junctions with RNA-Seq. *Bioinformatics*. 25:1105–1111.
- Tu, J., D. Fu, Y. Gu, Y. Shao, X. Song, M. Xue, and K. Qi. 2021. Transcription regulator *ygek* affects the virulence of avian pathogenic *Escherichia coli*. *Animals*. 11:1–12.
- Tu, J., B. Huang, Y. Zhang, Y. Zhang, T. Xue, S. Li, and K. Qi. 2016. Modulation of virulence genes by the two-component system PhoP-PhoQ in avian pathogenic *Escherichia coli*. *Pol. J. Vet. Sci.* 19:31–40.
- Wang, S., Y. Bao, Q. Meng, Y. Xia, Y. Zhao, Y. Wang, F. Tang, X. Zhuge, S. Yu, X. Han, J. Dai, and C. Lu. 2015. IbeR facilitates stress-resistance, invasion and pathogenicity of avian pathogenic *Escherichia coli*. *PLoS One*. 10:5–10.
- Wu, F. L., Y. Liu, H. N. Zhang, H. W. Jiang, L. Cheng, S. J. Guo, J. Y. Deng, L. J. Bi, X. E. Zhang, H. F. Gao, and S. C. Tao. 2018. Global profiling of PknG interactions using a human proteome microarray reveals novel connections with CypA. *Proteomics*. 18:1–25.
- Xi, D., Y. Li, J. Yan, Y. Li, X. Wang, and B. Cao. 2020. Small RNA *coaR* contributes to intestinal colonization in *Vibrio cholerae* via the two-component system EnvZ/OmpR. *Environ. Microbiol.* 22:4231–4243.
- Yi, Z., D. Wang, S. Xin, D. Zhou, T. Li, M. Tian, J. Qi, C. Ding, S. Wang, and S. Yu. 2019. The CpxR regulates type VI secretion system 2 expression and facilitates the interbacterial competition activity and virulence of avian pathogenic *Escherichia coli*. *Vet. Res.* 50:1–12.
- Yin, L., Q. Li, M. Xue, Z. Wang, J. Tu, X. Song, Y. Shao, X. Han, T. Xue, H. Liu, and K. Qi. 2019. The role of the *phoP* transcriptional regulator on biofilm formation of avian pathogenic *Escherichia coli*. *Avian Pathol.* 48:362–370.
- Yu, L., W. Li, K. Qi, S. Wang, X. Chen, J. Ni, R. Deng, F. Shang, and T. Xue. 2019. McbR is involved in biofilm formation and H₂O₂ stress response in avian pathogenic *Escherichia coli* X40. *Poult. Sci.* 98:4094–4103.
- Yu, L., H. Wang, X. Han, W. Li, M. Xue, K. Qi, X. Chen, J. Ni, R. Deng, F. Shang, and T. Xue. 2020. The two-component system, BasSR, is involved in the regulation of biofilm and virulence in avian pathogenic *Escherichia coli*. *Avian Pathol.* 49:532–554.
- Zhang, Y., Y. Wang, H. Zhu, Z. Yi, D. J. A. Afayibo, C. Tao, T. Li, M. Tian, J. Qi, C. Ding, S. Yu, and S. Wang. 2021. DctR contributes to the virulence of avian pathogenic *Escherichia coli* through regulation of type III secretion system 2 expression. *Vet. Res.* 52:1–12.